Finally, we consider the role that the Elav protein may play in the development of the neuron. The *elav* locus is not expressed in neuroblasts but is expressed in young neurons (*5*), and it continues to be expressed in neurons through all developmental stages (*5*). Although the *elav* gene function is not required to generate neurons, it is essential for the formation of a structurally normal embryonic central nervous system (*4*) and adult retina and optic lobe (*1, 2*). Given the probable RNA-binding capability of the Elav protein, we propose that the product (or products) of this locus provides a function essential for the RNA metabolism of all neurons. More specifically, we propose that the Elav protein is required for the proper posttranscriptional processing of transcripts of other genes that participate in neuronal maturation and maintenance.

REFERENCES AND NOTES

1. A. R. Campos, D. Grossman, K. White, *J. Neurogenet.* **2**, 197 (1985).
2. T. Homyk, Jr., K. Isono, W. L. Pak, *ibid.*, p. 309.
3. A. R. Campos, D. R. Rosen, S. N. Robinow, K. White, *EMBO J.* **6**, 425 (1987).
4. F. Jiménez and J. A. Campos-Ortega, *J. Neurogenet.* **4**, 179 (1987).
5. S. Robinow and K. White, *Dev. Biol.* **126**, 294 (1988).
6. M. S. Swanson, T. Y. Nakagawa, K. LeVan, G. Dreyfuss, *Mol. Cell. Biol.* **7**, 1731 (1987).
7. G. Dreyfuss, M. S. Swanson, S. Piñol-Roma, *Trends Biochem. Sci.* **13**, 86 (1988).
8. The sequence of the 9.2-kb genomic DNA fragment and cDNA-1 are available through GenBank under accession nos. M21152 and M21153, respectively, or on request to the authors. The translation of the 1449-nucleotide ORF is available through the National Biomedical Research Foundation (NBRF)–PIR database under accession no. A30030.
9. R. Breathnach, C. Benoist, K. O'Hare, F. Gannon, P. Chambon, *Proc. Natl. Acad. Sci. U.S.A.* **75**, 4853 (1978); S. M. Mount, *Nucleic Acids Res.* **10**, 459 (1982).
10. The GAGA sequence motif is bound by a factor that activates transcription of the *Drosophila engrailed* and *Ubx* genes [W. C. Soeller, S. J. Poole, T. Kornberg, *Genes Dev.* **2**, 68 (1988); M. D. Biggin and R. Tjian, *Cell* **53**, 699 (1988)].
11. The sequence $^{C}_{T}$GAG$^{C}_{T}$G is recognized by the Zeste protein, which activates transcription of the *Ubx* promoter [M. D. Biggin, S. Bickel, M. Benson, V. Pirrotta, R. Tjian, *Cell* **53**, 713 (1988)].
12. The 11 copies of the sequence $^{C}_{T}$GAG$^{C}_{T}$G, or its inverse, are distributed as follows: three are located 2.6-kb to 3.1-kb upstream from the 5′ end of cDNA-1, one begins ten nucleotides from the end of the first exon of cDNA-1, three more copies are clustered in the first intron within 165 nucleotides of each other, another three copies are dispersed in the second intron, and the last copy is in the third exon of cDNA-1 at postion −81.
13. J. Topol, D. M. Ruden, C. S. Parker, *Cell* **42**, 527 (1985); M. Ptashne, *A Genetic Switch: Gene Control and Phage Lambda* (Blackwell, Boston, 1986).
14. D. R. Cavener, *Nucleic Acids Res.* **15**, 1353 (1987).
15. S. Robinow, unpublished data.
16. A. R. Campos, thesis, Brandeis University, Waltham, MA (1988).
17. The *elav* cDNA-2 was isolated from an adult head cDNA library (provided by Y. Citri). DNA sequence analysis demonstrates that this cDNA contains the same 1449-nucleotide ORF as cDNA-1 (S. Robinow, unpublished observation). RNA transcribed from this cDNA clone was translated in vitro in a reticulocyte lysate and the protein generated comigrates with the protein product of cDNA-1 (S. Robinow, unpublished data).
18. E. Bier, L. Ackerman, S. Barbel, L. Jan, Y. N. Jan, *Science* **240**, 913 (1988).
19. By immunoblot analysis, MAb44C11 recognizes two different fusion proteins produced in *Escherichia coli*. Both of these fusion proteins express the 1449-nucleotide ORF. The only sequences common to these two proteins are those of the 1449-nucleotide ORF (S. Robinow, unpublished data).
20. S. A. Adam, T. Nakagawa, M. S. Swanson, T. K. Woodruff, G. Dreyfuss, *Mol. Cell. Biol.* **6**, 2932 (1986); A. B. Sachs, M. W. Bond, R. D. Kornberg, *Cell* **45**, 827 (1986); F. Cobianchi, D. N. SenGupta, B. Z. Zmudzka, S. H. Wilson, *J. Biol. Chem.* **261**, 3536 (1986).
21. B. Lapeyre *et al.*, *J. Biol. Chem.* **261**, 9167 (1986); D. K. Lahiri and J. O. Thomas, *Nucleic Acids Res.* **14**, 4077 (1986); T. Grange, C. Martins de Sa, J. Oddos, R. Pictet, *ibid.* **15**, 4771 (1987); A. Y.-S. Jong, M. W. Clark, M. Gilbert, A. Oehm, J. L. Campbell, *Mol. Cell. Biol.* **7**, 2947 (1987).
22. S. R. Haynes, M. L. Rebbert, B. A. Mozer, F. Forquignon, I. B. Dawid, *Proc. Natl. Acad. Sci. U.S.A.* **84**, 1819 (1987); L. R. Bell, E. M. Maine, P. Schedl, T. W. Cline, *Cell*, in press; T. Goralski and B. Baker, personal communication.
23. F. Sanger, S. Nicklen, A. R. Coulson, *Proc. Natl. Acad. Sci. U.S.A.* **74**, 5463 (1977); S. Henikoff, *Methods Enzymol.* **155**, 156 (1987). Sequence analysis was accomplished with the DNA Inspector II+ DNA analysis program (Textco).
24. U. K. Laemmli, *Nature* **227**, 680 (1970).
25. L. G. Davis, M. D. Dibner, J. F. Battey, *Basic Methods in Molecular Biology* (Elsevier, New York, 1986), pp. 311–314.

26. We thank E. Bier, L. Jan, and Y. N. Jan for generously supplying monoclonal antibody MAb44C11, and M. Rosbash for getting us started on the protein analysis. We are grateful to L. L. Restifo and J. C. Hall for comments and suggestions concerning this manuscript. Supported by NIH grant GM-33205.

16 August 1988; accepted 19 October 1988

Lineage-Specific Development of Calcium Currents During Embryogenesis

LUCIANA SIMONCINI, MELODYE L. BLOCK, WILLIAM J. MOODY

The development of electrophysiological properties of isolated, identified ascidian blastomeres was followed from the fertilized egg to the neurula, and the stage at which cells of different lineages first express different functional ion channel populations was determined. Little has been known about such events because of the difficulties of making voltage-clamp recordings from small embryonic cells and of identifying their developmental fates in dissociated preparations. The problem of small cell size was circumvented by using the whole-cell patch clamp, and identification was facilitated by the use of a species of ascidian, *Boltenia villosa*, in which endogenous pigment marks cells of specific developmental fates. Within approximately 3 hours after gastrulation, muscle-lineage blastomeres in these embryos developed a voltage-dependent calcium current while surrounding blastomeres of other lineages did not. At about the same time, all cells developed delayed outward potassium currents and lost the inwardly rectifying potassium currents present at earlier stages.

THE MECHANISMS BY WHICH CELLS of different developmental fates acquire their characteristic electrical properties during embryogenesis are poorly understood. Later stage blastomeres are difficult to isolate and record from if conventional microelectrode techniques are used. It is also difficult in most preparations to identify the developmental fates of cells that have been separated from the embryo. A number of earlier studies have used cytochalasin B to

Department of Zoology, University of Washington, Seattle, WA 98195.

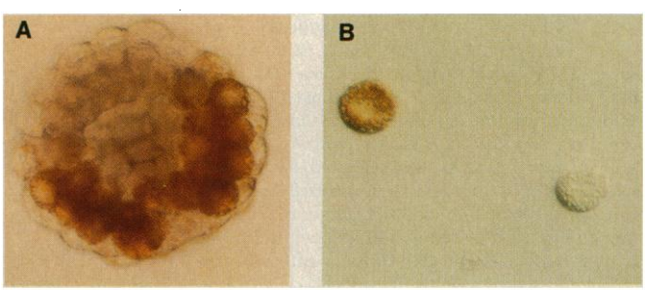

Fig. 1. (**A**) Photograph of a *Boltenia* embryo at the gastrula stage, approximately 13 hours after fertilization. The embryo is viewed from the dorsal aspect, showing the blastopore, with the left-right axis of symmetry running from upper left (anterior) to lower right (posterior). The diameter of the gastrula is about 150 μm. Muscle-lineage cells lie along the posterior rim of the blastopore and are easily recognized by their endogenous orange pigment. (**B**) Two cells dissociated from the gastrula and photographed under differential interference contrast optics. The muscle-lineage cell can be distinguished by its orange color but is otherwise similar in morphology to its nonmuscle neighbor. The cells are about 30 μm in diameter.

block cytokinesis so that the development of large, early-stage cells could be studied without further cleavages (*1*). Although the use of this technique solves the problem of size, it changes some aspects of cell differentiation, because the cleavages that separate lineage determinants do not occur. We have applied the whole-cell clamp (*2*) to blastomeres isolated at various stages of embryogenesis in the ascidian *Boltenia villosa*. Ascidians are primitive marine chordates (subphylum Urochordata; commonly known as sea squirts) whose embryos display a pronounced form of mosaic development; cell lineages are established early in embryogenesis, and fate maps for the embryo are well described (*3, 4*). In *Boltenia*, muscle-lineage cells carry an intense orange pigment that enables them to be identified at any stage of development, even in dissociated preparations (Fig. 1) (*5*). This endogenous visual marker of cell fate has allowed us to compare the development of ion channel populations in muscle- and nonmuscle-lineage cells at early stages when these cell types are otherwise morphologically indistinguishable.

We previously described electrophysiological changes that occurred between fertilization and the eight-cell stage (*6*). The unfertilized *Boltenia* oocyte has three major voltage-dependent currents, carried through Na^+ and Ca^{2+} channels, activated by depolarization, and inwardly rectifying K^+ channels, activated at potentials negative to rest. The Na^+ current virtually disappeared from all blastomeres by the eight-cell stage, whereas both the Ca^{2+} and the inwardly rectifying K^+ currents were maintained at oocyte densities in all blastomeres through the eight-cell stage. Thus all blastomeres through the eight-cell stage are similar in their electrical properties (*7*).

In the present studies, we have extended these experiments to the gastrula and neurula stages of development (*8*). All cells in the gastrula showed very uniform electrical properties, although they differed from cells of the eight-cell embryo (Fig. 2). The Ca^{2+} current was greatly decreased from eight-cell-stage levels and was undetectable in most gastrula cells (Fig. 2A). The inward rectifier, on the other hand, was present in all gastrula cells at about the same density as at the eight-cell stage (Fig. 2B).

During the approximately 3 hours in which the gastrula develops into the neurula, several changes took place that dramatically altered the electrical properties of cells isolated from the neurula.

1) Large Ca^{2+} currents appeared in muscle-lineage cells but not in blastomeres of the nonmuscle lineages (Figs. 2A and 3A). The neurula was thus the first stage at which we could detect lineage-specific differences in ion channel populations. The Ca^{2+} currents appeared before any obvious changes in cell morphology.

2) The inward rectifier was greatly reduced in all neurula-stage cells irrespective of lineage (Figs. 2B and 3B).

3) Delayed outward K^+ currents, which were not seen in significant amounts at any earlier stages of development, appeared in both muscle- and nonmuscle-lineage cells of the neurula (*9*) (Fig. 4). Reliable detection of the Ca^{2+} current in muscle-lineage cells from the neurula required the elimination of the delayed K^+ current by substitution of internal Cs^+ for K^+.

The Ca^{2+} current in muscle-lineage cells from the neurula was very similar to the oocyte Ca^{2+} current (*6*). Both were activated at potentials positive to −20 mV with peak currents at +10 to +20 mV. Both showed the permeability sequence $Ba^{2+}>Sr^{2+}>Ca^{2+}$ and had greatly slowed inactivation with either Ba^{2+} or Sr^{2+} as the permeant ion, implying Ca^{2+}- rather than voltage-dependent inactivation (*10*). The current density, however, was about ten times higher at the neurula stage than in the oocyte or in eight-cell-stage blastomeres.

To determine whether the appearance of

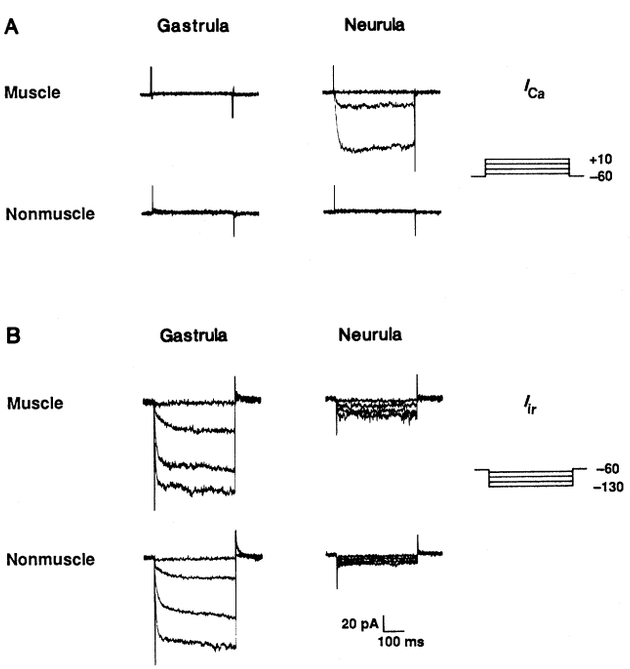

Fig. 2. Whole-cell currents in muscle- and nonmuscle-lineage blastomeres at gastrula and neurula stages of embryogenesis. (**A**) Ca^{2+} currents. Holding potential, −60 mV; steps to −50, −30, −10, and +10 mV. Ionic conditions: Cs^+-int, Ba^{2+}-ASW (*8*). Between the gastrula and neurula stages, a period of about 3 hours, muscle-lineage blastomeres developed Ca^{2+} currents while nonmuscle-lineage cells did not. Depolarizing steps from more negative holding potentials did not reveal a voltage-dependent Na^+ current in any of the blastomeres at either stage. (**B**) Inwardly rectifying K^+ current. Holding potential, −60 mV; steps to −70, −90, −110, and −130 mV. Ionic conditions: K^+-int, Sr^{2+}-ASW. Between the gastrula and neurula stages, both muscle- and nonmuscle-lineage blastomeres lost the inwardly rectifying K^+ current. The time and voltage calibrations apply to all records. The records are not corrected for leakage currents or capacitative transients.

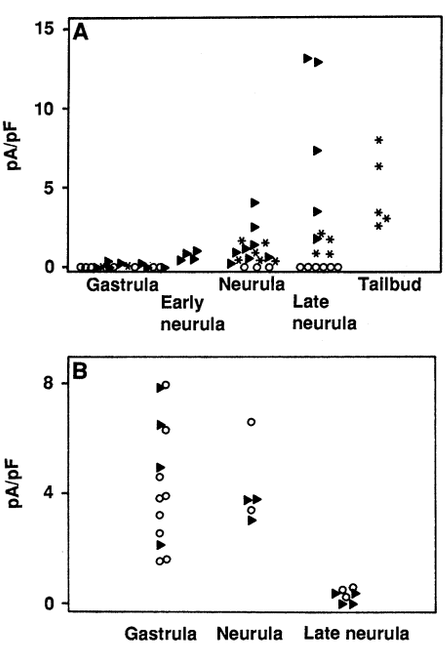

Fig. 3. (**A**) Development of the Ca^{2+} current in cells of muscle (▶) and nonmuscle (○) lineage dissociated from embryos of the stage indicated, or from muscle-lineage cells dissociated at the gastrula stage and allowed to develop as isolated cells until control embryos reached the stage indicated (⋆). At the gastrula stage ▶ and ⋆ symbols represent the same experimental paradigm. Each point represents the maximum current density in picoamperes of current per picofarad of capacitance in a single blastomere. All currents were measured from a holding potential of −60 mV in Ba^{2+}-ASW (external solution) with Cs^+-int used in the pipette (*8*). (**B**) The inwardly rectifying K^+ current density (same symbols) in picoamperes per picofarad for single blastomeres. Currents were measured at −130 mV from a holding potential of −60 mV in Sr^{2+}-ASW (external solution) with K^+-int used in the recording pipette. Cell capacitance was measured by applying a 10-mV, 50-Hz triangle wave command to the voltage-clamp amplifier and measuring the amplitude of the resulting square-wave current signal.

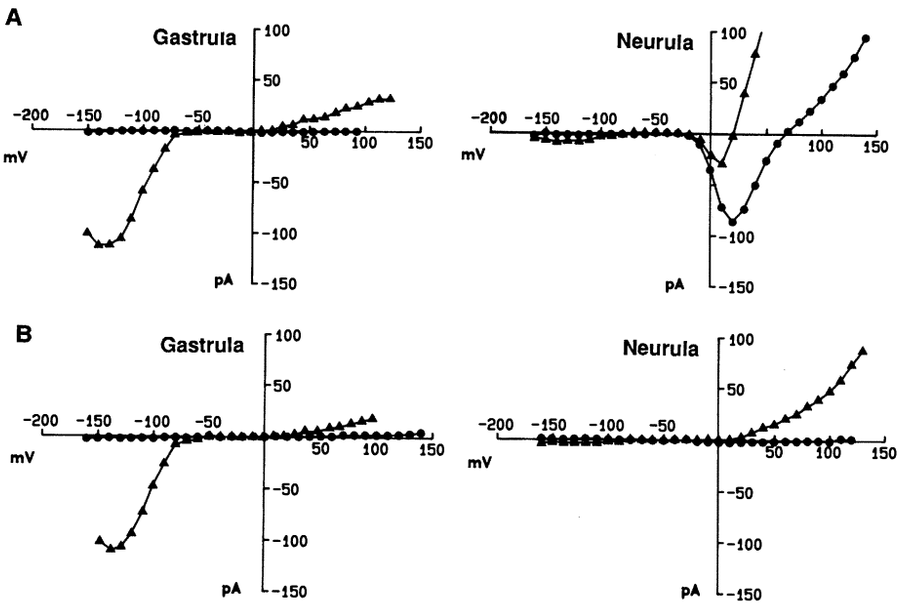

Fig. 4. Current-voltage (*I-V*) relations for (**A**) muscle- and (**B**) nonmuscle-lineage cells at gastrula and neurula stages. Each panel shows two I-V relations, one in Cs^+-int/Ba^{2+}-ASW (●) to block outward K^+ currents and maximize detection of Ca^{2+} currents; the other in K^+-int/Sr^{2+}-ASW (▲) to maximize outward and inwardly rectifying K^+ currents; Sr^{2+} was used instead of Ca^{2+} because it gave larger currents through Ca^{2+} channels, so that we could better estimate the overlap between inward and outward currents, but did not block the inward rectifier, like Ba^{2+}. All points were taken from a holding potential of −60 mV and represent steady-state currents (the Ca^{2+} current does not inactivate with Sr^{2+} or Ba^{2+} as the permeant ion). The decrease of inwardly rectifying K^+ current at very negative potentials is probably due to block by external Sr^{2+} or Na^+ ions. In the Cs^+-int/Ba^{2+}-ASW solution, muscle neurula cells showed substantial outward currents that probably represent Cs^+ efflux through the Ca^{2+} channels (*17*). We have corrected these plots by subtracting the extrapolated linear leakage currents recorded between −60 and −40 mV, where no voltage-sensitive currents are present. The off-scale delayed K^+ current points in the muscle neurula plot with internal K^+ (▲) are: +50 mV, 120 pA; +80 mV, 221 pA; and +100 mV, 296 pA.

Ca^{2+} currents in muscle-lineage cells after gastrulation required cell contacts during this period, we dissociated cells from early gastrulae, well before Ca^{2+} currents could be detected, and allowed them to develop as individual cells. Data from these cells (Fig. 3A) showed that Ca^{2+} currents developed approximately on schedule, with perhaps a slight delay relative to cells in intact embryos. This result indicates that at least the terminal phase of Ca^{2+} current development is an autonomous function of muscle-lineage cells.

We can now divide early *Boltenia* embryogenesis into two phases on the basis of the sequence of changes in ion channel populations occurring in the blastomeres. The first phase, from fertilization to just after gastrulation, is characterized by uniformity in the electrical properties of blastomeres of different developmental fates and by the sequential loss of currents present in the oocyte. The second phase, which begins just after gastrulation, is characterized by differences in ion channel populations between cells of different lineages and by the appearance of currents not seen in the oocyte (*11*).

The development of Ca^{2+} currents seems to be one of the earliest events in the terminal differentiation of ascidian muscle, occurring at about the same time as acetylcholinesterase and myosin adenosine triphosphatase synthesis (*12, 13*) but preceding innervation, acetylcholine receptor appearance (*14*), contractility, and changes in cell morphology (*15*). Because the Ca^{2+} currents appear well before they play a role in contractility, they may have some as yet unknown function in terminal differentiation of muscle cells in the larva (*16*).

The fact that the muscle-specific development of Ca^{2+} currents occurs over the same time period as the changes in two K^+ currents common to all lineages may allow the developmental cues for these types of events to be separated. The principles elucidated from such studies in this preparation may be widely applicable to the question of how the electrical properties of cells develop during embryogenesis.

REFERENCES AND NOTES

1. K. Takahashi and M. Yoshii, *J. Physiol. (London)* **315**, 515 (1981); T. Hirano, K. Takahashi, N. Yamashita, *ibid.* **347**, 301 (1984); T. Hirano and K. Takahashi, *ibid.*, p. 327; *ibid.* **386**, 113 (1987).
2. O. P. Hamill, A. Marty, E. Neher, B. Sakmann, F. J. Sigworth, *Pfluegers Arch.* **391**, 85 (1981).
3. G. Ortolani, *Acta Embryol. Morphol. Exp.* **1**, 247 (1958); W. R. Jeffery and S. Meier, *Dev. Biol.* **96**, 125 (1983); E. G. Conklin, *J. Acad. Nat. Sci. Philadelphia* **13**, 1 (1905); G. Reverberi, in *Experimental Embryology of Marine and Freshwater Invertebrates*, G. Reverberi, Ed. (American Elsevier, New York, 1971), pp. 507–550; J. R. Whittaker, in *Determinants of Spatial Organization*, S. Subtelny and I. R. Konigsberg, Eds. (Academic Press, New York, 1979), pp. 29–51; *Dev. Biol.* **93**, 463 (1982).
4. H. Nishida and N. Satoh, *Dev. Biol.* **99**, 382 (1983); *ibid.* **110**, 440 (1985).
5. W. R. Jeffery, *Science* **216**, 545 (1982).
6. M. L. Block and W. J. Moody, *J. Physiol. (London)* **393**, 619 (1987).
7. The maintenance of Ca^{2+} current and inward rectifier density occurred in spite of a threefold increase in surface area between fertilization and the eight-cell stage, implying the addition of functional channels of both types to the embryo along with new membrane. The similarity of blastomere electrical properties at the eight-cell stage is significant in that determinants for some major tissue types have been segregated into different cells by this time.
8. Animal handling, gamete preparation and fertilization, electrophysiological methods, and data acquisition were as described in (*6*). Chorions were removed manually from embryos that had reached the desired stage of development with electrolytically sharpened tungsten needles. Cells were dissociated either manually or by incubation for 5 to 15 min in a low-Ca^{2+} collagenase medium containing 460 m*M* NaCl, 10 m*M* KCl, 0.5 m*M* $CaCl_2$, 10 m*M* Hepes, *p*H 7.5, and collagenase (1 mg/ml) (Sigma type IV). Cells were then returned to the appropriate external solution for recording and lightly triturated to facilitate their dispersion. In some experiments (see text), cells were isolated from gastrula-stage embryos and allowed to develop in the absence of contacts with other blastomeres. In these cases, the isolated cells developed in ASW and were placed in Ba^{2+}-ASW (see below) at the beginning of the recording session. Staging of embryos (hours after fertilization, 10°C): eight-cell (3.5), gastrula (13), neurula (16), hatching (36). We cannot be certain that all nonmuscle lineages were sampled, because they are all unpigmented and difficult to distinguish. However, inasmuch as our sample included 30 nonmuscle cells (19 embryos) and these cells had a wide range of morphologies, diameters, and surface areas (determined by capacitance), we believe that at least several of the major nonmuscle lineages [for example, endoderm, notochord, nervous system, epidermis, mesenchyme (*2*)] were included.

   External solutions: Artificial seawater (ASW) contained 400 m*M* NaCl, 10 m*M* KCl, 10 m*M* $CaCl_2$, 50 m*M* $MgCl_2$, 10 m*M* Hepes, *p*H 8.0 to 8.1; Ba^{2+}-ASW contained 50 m*M* $BaCl_2$ and 10 m*M* $MgCl_2$ instead of 10 m*M* $CaCl_2$ and 50 m*M* $MgCl_2$; Sr^{2+}-ASW contained 50 m*M* $SrCl_2$ and 10 m*M* $MgCl_2$ instead of 10 m*M* $CaCl_2$ and 50 m*M* $MgCl_2$. Internal solutions: K^+-int contained 400 m*M* KCl, 10 m*M* NaCl, 1 m*M* $MgCl_2$, 10 m*M* EGTA, 20 m*M* Hepes, 2 m*M* theophylline, 0.1 m*M* adenosine 3′,5′-monophosphate, 2 m*M* Mg adenosine 3′,5′-triphosphate, *p*H 7.3; Cs^+-int contained 400 m*M* CsCl substituted for 400 m*M* KCl.
9. Delayed K^+ currents tended to be larger in muscle than in nonmuscle cells. We have not explored this difference further.
10. Compare the present data to figure 1 in (*6*). These similarities are significant in light of the report that Ca^{2+} currents in cleavage-arrested embryos of the ascidian *Halocynthia roretzi* differ from oocyte currents in both permeability sequence and inactivation mechanism (*1*).
11. In phase I the Na^+ current and the inward rectifier current disappear rather abruptly: the Na^+ current in the 2 hours between fertilization and first cleavage, and the inward rectifier current in about 3 hours between gastrula and neurula. We do not know the time course of the loss of the Ca^{2+} current between the eight-cell stage and the gastrula. The beginning of phase II overlaps the end of phase I, because the Ca^{2+} current density begins to increase before the inward rectifier disappears.
12. T. H. Meedel and J. R. Whittaker, *Proc. Natl. Acad. Sci. U.S.A.* **80**, 4761 (1983).

13. T. H. Meedel, *J. Exp. Zool.* **227**, 203 (1983).
14. H. Ohmori and S. Sasaki, *J. Physiol. (London)* **269**, 221 (1977).
15. L. Simoncini, M. L. Block, W. J. Moody, unpublished data.
16. Larval muscle in the ascidian *Halocynthia* generates a Ca^{2+}-dependent action potential with a rapid repolarizing phase (*14*), so the currents we record at the neurula stage probably approximate those found in fully differentiated muscle. We have not yet recorded from mature larval *Boltenia* muscle. Muscle-lineage cells in *Halocynthia* that were cleavage-arrested at early stages and allowed to develop until control embryos reached the larval stage showed Ca^{2+} and delayed K^+ currents (*1*).
17. K. S. Lee and R. W. Tsien, *Nature* **297**, 498 (1982); W. Almers, E. W. McClesky, P. T. Palade, *J. Physiol. (London)* **353**, 565 (1984); P. Hess and R. W. Tsien, *Nature* **309**, 453 (1984).
18. We thank J. Palka, K. Graubard, and M. Bosma for critical reading of the manuscript. Supported by NIH grant HD17486, a Research Career Development Award to W.J.M., and NIH postdoctoral fellowship NS07775 to M.L.B.

3 June 1988; accepted 11 October 1988

Grafting Genetically Modified Cells to the Damaged Brain: Restorative Effects of NGF Expression

MICHAEL B. ROSENBERG, THEODORE FRIEDMANN, ROBIN C. ROBERTSON, MARK TUSZYNSKI, JON A. WOLFF,* XANDRA O. BREAKEFIELD, FRED H. GAGE†

Fibroblasts were genetically modified to secrete nerve growth factor (NGF) by infection with a retroviral vector and then implanted into the brains of rats that had surgical lesions of the fimbria-fornix. The grafted cells survived and produced sufficient NGF to prevent the degeneration of cholinergic neurons that would die without treatment. In addition, the protected cholinergic cells sprouted axons that projected in the direction of the cellular source of NGF. These results indicate that a combination of gene transfer and intracerebral grafting may provide an effective treatment for some disorders of the central nervous system.

CONSIDERABLE EFFORT IN RECENT years has been applied toward the development of methods for the genetic modification of mammalian cells to correct disease phenotypes in vivo. Because of their accessibility, cells of the bone marrow and skin have been studied most extensively. Because of its relative inaccessibility, a very important target organ, the brain, has received little attention. The development of methods for intracerebral neural grafting has provided new approaches towards the treatment of central nervous system (CNS) disorders. We have previously suggested that a combination of the gene transfer and neural grafting may constitute an effective approach to therapy in the CNS (*1*). Specifically, we have demonstrated that cultured cells genetically modified with retroviral vectors can survive when implanted in the mammalian brain and can continue to express foreign gene (transgene) products (*1, 2*). Before this approach can be used to treat specific CNS diseases, one prerequisite is to determine whether, under any circumstances, sufficient transgene product can be made in vivo to complement or repair an absent or previously damaged brain function.

To test the potential of this therapeutic approach, we have chosen a well-characterized model that provides the opportunity to observe a functional effect. After transection of the fimbria-fornix (the pathway connecting cholinergic neurons of the basal forebrain to their target in the hippocampus), many of the cholinergic neurons undergo retrograde degeneration, exhibit a decrease in the activities of many enzymes, and, in some cases, die (*3, 4*). This degenerative response is attributed to the loss of trophic support from β–nerve growth factor (NGF), which is normally transported retrogradely in the intact brain from the hippocampus to the septal cholinergic cell bodies (*5–10*). The importance of NGF in this response to damage is supported by experiments that demonstrate that cholinergic neurons in the medial septum can be protected from retrograde degeneration by chronic infusion of exogenous NGF (*11–14*). We report here that cultured fibroblasts, genetically modified to produce and secrete NGF and then grafted to the cavity formed in creating a fimbria-fornix lesion, will prevent retrograde cholinergic degeneration and induce axonal sprouting, thereby demonstrating a functional response to the grafted cells.

A retroviral vector, similar to one described previously (*15*), was constructed from Moloney murine leukemia virus (*16*). It contains the 777-bp Hga I–Pst I fragment of mouse NGF cDNA (*17, 18*) under control of the viral 5′ long terminal repeat. This insert corresponds to the shorter NGF transcript that predominates in mouse tissue receiving sympathetic innervation (*19*) and is believed to encode the precursor to NGF that is secreted constitutively. The vector also includes a dominant selectable marker encoding the neomycin-resistance function of transposon Tn5 (*20*) under control of an internal Rous sarcoma virus promoter. Transmissible retrovirus was produced by transfecting vector DNA into PA317 amphotropic producer cells (*21*) by the calcium phosphate co-precipitation method (*22*) and by using medium from these cells to infect Ψ2 ecotropic producer cells (*23*) in the presence of Polybrene (Sigma; 4 μg/ml). Virus from the Ψ2 clone producing the highest titer (4×10^5 colony-forming units per milliliter), was used to infect the established rat fibroblast cell line 208F (*24*) as described (*25*). Individual neomycin-resistant colonies, selected in medium containing the neomycin analog G418, were expanded and tested for NGF production and secretion by a two-site enzyme immunoassay, with commercially available reagents according to the manufacturer's protocol (Boehringer Mannheim). The clone producing the highest levels of NGF contained 1.7 ng of NGF per milligram of total cellular protein and secreted NGF into the medium at a rate of 50 pg/hour per 10^5 cells. The NGF secreted by this clone was biologically active, as determined by its ability to induce neurite outgrowth from PC12 rat pheochromocytoma cells (*26, 27*). Uninfected 208F cells, in contrast, did not produce detectable levels of NGF in either assay.

Fimbria-fornix lesions were made in 16 rats; 8 rats received grafts of infected cells and the remaining 8 received uninfected control cells (*28*). After 2 weeks, all animals were killed and processed for immunohistochemistry (*28*). Staining for fibronectin, a fibroblast-specific marker, revealed robust graft survival in all 16 animals that was comparable in both groups (Fig. 1, A and B). Sections stained for choline acetyltransferase (ChAT) to evaluate the survival of cholinergic cell bodies indicated a greater number of remaining neurons on the lesioned side of the medial septum in all 8 animals that had received grafts of infected

M. B. Rosenberg, T. Friedmann, J. A. Wolff, Department of Pediatrics and Center for Molecular Genetics, M-034, University of California School of Medicine, La Jolla, CA 92093.
R. C. Robertson, M. Tuszynski, F. H. Gage, Department of Neurosciences, M-024, University of California School of Medicine, La Jolla, CA 92093.
X. O. Breakefield, Molecular Neurogenetics, E. K. Shriver Center, Waltham, MA 02254; Laboratory of Neurogenetics, Massachusetts General Hospital, Boston, MA 02114; and Neuroscience Program (Neurology), Harvard Medical School, Boston, MA 02115.

*Present address: Departments of Pediatrics and Genetics, Waisman Center, University of Wisconsin, Madison, WI 53792.
†To whom correspondence should be addressed.